

Diversity in the reactions of unsymmetric dinucleating Schiff base ligands with Cu^{II} and Ni^{II}

Harry Adams,^a David E. Fenton,^{*a} Shabana R. Haque,^a Sarah L. Heath,^a Masaaki Ohba,^b Hisashi Okawa^b and Sharon E. Spey^a

^a Department of Chemistry, Dainton Building, The University of Sheffield, Sheffield, UK S3 7HF

^b Department of Chemistry, Faculty of Science, Kyushu University, Hakozaki, Higashiku, Fukuoka 812, Japan

Received 21st February 2000, Accepted 20th April 2000

Published on the Web 23rd May 2000

A diversity of reaction products have been found in the reactions of two related unsymmetrical Schiff base dinucleating ligands, **HL**¹ and **HL**², derived from 3-chloromethyl-5-methylsalicylaldehyde **1**, with copper(II) and nickel(II) salts. The ligands remain intact in the copper(II) complexes to give the homodinuclear complexes [Cu₂L¹Br₃] **2** and [Cu₂L²-(OH)(ClO₄)ClO₄] **3**, the crystal structures of which have been solved. The reactions of **HL**¹ and **HL**² with nickel perchlorate led to hydrolysis of the imine bond. With **HL**¹ the homodinuclear complex [NiL¹(OH₂)₂][ClO₄]₂·4H₂O was formed and with **HL**² hydrolysis was followed by elimination of C₂H₄ from the terminal NET₂ of the iminic side arm to leave an NHET group and the dinuclear complex [NiL²(OH₂)₂][ClO₄]₂·3CH₃OH. The crystal structures of the two nickel complexes are also reported.

Introduction

Current awareness of the asymmetric nature of a number of homodinuclear or heterodinuclear transition metal-derived metallobiosites and of the ability of the individual metal ions to have quite distinct roles in the functioning of the metallo-enzyme concerned has led to a search for carefully designed unsymmetric dinucleating ligands which will give dinuclear complexes capable of acting as models for the metallobiosites.^{1,2}

The biosites in question have been classified in four distinct groupings as follows (Fig. 1):³ (a) symmetric, in which an identical number of donor atoms of the same type are bound to each metal atom in similar geometries; (b) donor asymmetry, where different types of donor atom co-ordinate to each metal atom; (c) geometric asymmetry, where there are inequivalent geometric arrangements of the donor atoms about each metal atom; and (d) co-ordination number asymmetry, where a different number of donor atoms are co-ordinated to each metal atom. To a first approximation the nature of the donor atom may be restricted to simply O, N, S, *etc.* but a more accurate definition would specify the functional grouping associated

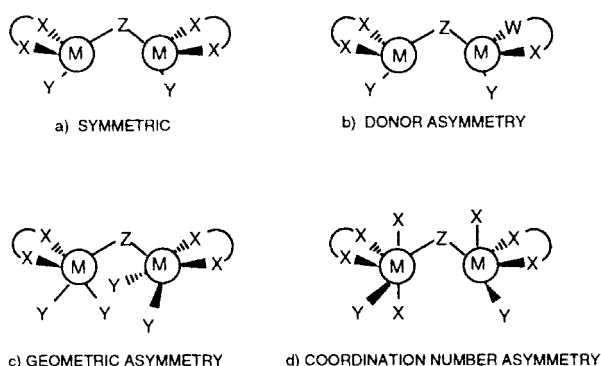


Fig. 1 A classification of metal co-ordination environments found at transition metal-derived dinuclear centres present in metallobiosites (M is a transition metal and W, X, Y and Z are ligand donor atoms such as N, O, S, *etc.*).

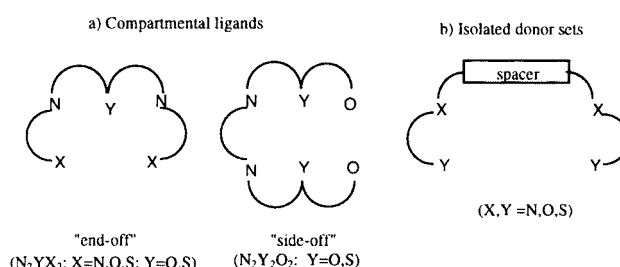


Fig. 2 Schematic representations of dinucleating ligands. Mono- or bi-bracchial pendant arms may be attached to the N atoms in the “end-off” compartmental ligands and to the X atoms in the isolated donor sets. The spacers in the isolated donor sets do not provide bridging atoms.

with the donor atom and so differentiate between an oxygen atom in water and carboxylate or a sulfur atom in a thiolate or a thioether. A combination of different types of asymmetry may also occur at a dinuclear centre.

Although many examples of co-ordination complexes derived from symmetric acyclic dinucleating ligands have been prepared and investigated as potential model complexes for metallobiosites, polydentate ligand systems that would give necessarily asymmetric dinuclear complexes remain rare; site asymmetry was often only accessed through good fortune. Complexes of dinucleating ligands have been divided into two general classes (Fig. 2).⁴ The first group consists of those complexes in which the metals share at least one donor atom in species containing adjacent sites in which the central donor atom(s) provide a bridge; the ligands giving these ‘bridging donor sets’ have collectively been termed compartmental ligands. The second group consists of those complexes in which donor atoms are not shared and so isolated donor sets exist. If the arms are constituted of different donor atoms then an unsymmetric ligand results.

Early studies on the derivation of unsymmetric “end-off” compartmental proligands involved the introduction of a single pendant arm into a 5-substituted salicylaldehyde, using the

Mannich reaction, followed by condensation of the resulting aminomethyl salicylaldehyde with a primary amine to give a range of unsymmetric dinucleating Schiff base proligands and their dinuclear copper(II) complexes.^{5–7} More recently a synthetic route based on the reaction of 3-chloromethyl-5-methylsalicylaldehyde (**1**) with functionalised secondary amines followed by Schiff base condensation with functionalised primary amines has provided a further range of unsymmetric proligands.^{8,9} In the current work the functionalised secondary amines *N*-ethyl-*N'*,*N'*-dimethylethane-1,2-diamine and *N,N*-diethyl-*N'*-methylethane-1,2-diamine were used to prepare the proligands **HL^A** and **HL^B**; *N,N*-dimethylethane-1,2-diamine was then used to prepare the donor asymmetric compartmental ligands **HL¹** and **HL²**, the asymmetry arising from the mixture of sp² and sp³ N atoms available for metal co-ordination. The ligands were then treated with copper(II) and nickel(II) to derive homodinuclear complexes.

Experimental

Elemental analyses were carried out by the University of Sheffield microanalytical service. Infrared spectra were recorded as KBr discs or as liquid films between NaCl plates, using a Perkin-Elmer 297 (4000–600 cm⁻¹) or a 1600 (4000–400 cm⁻¹) infrared spectrophotometer, ¹H and ¹³C NMR spectra using either a Bruker ACF-250, AM-250 or WH-400 spectrometer and positive ion fast atom bombardment (FAB) mass spectra using a Kratos MS80 or a VG PROSPEC spectrometer (the matrix used was 4-nitrobenzyl alcohol).

Ligand synthesis

3-Chloromethyl-5-methylsalicylaldehyde was prepared by the method of reference 8.

Precursor HL^A. 3-Chloromethyl-5-methylsalicylaldehyde (1.0 g, 5.43 mmol) was stirred at 0 °C in THF (75 ml). *N*-Ethyl-*N'*,*N'*-dimethylethane-1,2-diamine (1.71 cm³, 10.9 mmol) was added dropwise, over approximately 45 minutes, *via* a dropping funnel. The solution immediately turned bright yellow and was stirred for a further hour at 0 °C. The orange reaction mixture was filtered to remove any hydrochloride salt, then THF was removed from the filtrate *in vacuo* to give an oily orange solid which was first dissolved in distilled water (25 cm³) to which chloroform (25 cm³) was added. The washings were poured into a beaker and both layers acidified with HCl (2 M) to pH 1–2, causing the aqueous layer to become decolourised. The aqueous layer was removed and the pale yellow chloroform layer then made strongly basic with NaOH (10 M). The addition of base caused a bright yellow solid to be precipitated. The product was extracted with chloroform (4 × 25 cm³), the organic extracts were combined, dried with anhydrous magnesium sulfate, filtered and the filtrate evaporated to dryness giving a dark orange-yellow oil which was dried under vacuum. The oil was characterised using NMR and this revealed that there was no need for further purification. Yield = 65%. Found (required for C₁₅H₂₄N₂O₂): C, 67.69 (68.41); H, 9.25 (8.80); N, 10.49 (10.64)%. ¹H NMR (250 MHz, CDCl₃): δ 10.40 (1 H, s, CHO), 8.45 (1 H, broad s, phenolic proton), 7.45 (1 H, s, aryl CH), 7.00 (1 H, s, aryl CH), 3.60 (2 H, s, CH₂C₆H₂), 2.60 (4 H, q, NCH₂CH₃ and 2 H, t, EtNCH₂CH₂NMe₂), 2.55 (2 H, t, EtNCH₂CH₂NMe₂), 2.50 (2 H, q, NCH₂CH₃), 2.20 (3 H, s, NMe₂ and 3 H, s, CH₃C₆H₂) and 1.05 (3 H, t, NCH₂CH₃). ¹³C NMR (250 MHz, CDCl₃): δ 191.4 (CO), 159.9 (aryl), 136.4 (aryl), 127.7 (aryl), 127.4 (aryl), 124.6 (aryl), 56.5, 55.1, 50.0, 47.3, 45.3 (NMe₂), 20.2 (NMe) and 10.9 (C₆H₂Me). IR (NaCl plates): 3480 (ν_{OH}), 2969, 2819 (ν_{C-H, aliphatic}) and 1678 cm⁻¹ (ν_{C=O}). MS (FAB⁺): *m/z* 264 (25%, [C₁₅H₂₄N₂O₂]⁺).

Unsymmetrical Schiff base proligand HL¹. The proligand **HL^A** (0.22 g, 0.836 mmol) was gently refluxed in absolute

ethanol (25 cm³) for 10 minutes and *N,N*-dimethylethane-1,2-diamine (0.092 ml, 0.836 mmol) added to the boiling solution *via* a microsyringe. The solution instantly changed from a pale to bright yellow and was stirred for 10 minutes at room temperature. The solution was cooled in ice and the solvent removed *in vacuo* giving a bright orange-yellow oil. This was dried under high vacuum. Yield = 95%. Found (required for C₁₉H₃₄N₄O): C, 67.51 (68.22); H, 10.57 (10.25); N, 16.49 (16.75)%. ¹H NMR (250 MHz, CDCl₃): δ 8.35 (1 H, s, CHN), 7.20 (1 H, s, aryl CH), 7.00 (1 H, aryl s, CH), 3.70 (2 H, t, EtNCH₂CH₂NMe₂), 3.65 (2 H, s, CH₂C₆H₂), 2.65 (2 H, t, imine CH₂CH₂NMe₂), 2.65 (2 H, t, imine CH₂CH₂NMe₂), 2.60 (2 H, t, NEtCH₂CH₂NMe₂), 2.50 (2 H, t, EtNCH₂CH₂NMe₂), 2.50 (4 H, q, NCH₂CH₃), 2.40 (6 H, s, NMe₂, unsaturated pendant arm), 2.30 (3 H, s, CH₃C₆H₂), 2.15 (6 H, s, NMe₂, saturated pendant arm), 2.20 (3 H, s, NMe) and 1.10 (3 H, t, NCH₂CH₃). ¹³C NMR (250 MHz, CDCl₃): δ 164.7 (CN), 157.2 (aryl), 133.7 (aryl), 129.5 (aryl), 126.3 (aryl), 118.6 (aryl), 60.0, 57.9, 57.3, 52.1, 51.3, 47.9, 45.8 (NMe₂), 20.4 (C₆H₂Me) and 11.2 (NEt). IR (NaCl plates): 2940, 2857, 2815 (ν_{C-H, aliphatic}) and 1632 cm⁻¹ (ν_{C=N}). MS (FAB⁺): *m/z* 335 (95%, [C₁₉H₃₅N₄O]⁺).

Precursor HL^B. 3-Chloromethyl-5-methylsalicylaldehyde (1.42 g, 0.772 mmol) was dissolved in THF (50 cm³) at 0 °C. *N,N*-Diethyl-*N'*-methylethane-1,2-diamine (2.50 cm³, 1.54 mmol) was predissolved in THF (15 cm³), and then added dropwise to the stirring chloroaldehyde over a period of approximately one hour. On addition of the amine there was an immediate change from colourless to yellow and a cream precipitate deposited on the sides of the flask. The solution was stirred for a further hour at 0 °C. The solvent was removed *in vacuo* giving a red solid. The flask containing the solid was first washed with distilled water (20 cm³), and then chloroform (20 cm³). In each case the washings were poured into a beaker giving rise to two layers; an aqueous top layer and an organic bottom layer. Both layers were then acidified with HCl (2 M), causing a small amount of the precipitate found in the aqueous phase to dissolve. The aqueous phase was removed and made strongly basic with NaOH (10 M) (pH 10–11). On addition of base a yellow solid precipitated. The bright yellow solution was then extracted with chloroform (4 × 25 cm³), the organic extracts were combined, dried over anhydrous magnesium sulfate, filtered and then the filtrate was evaporated to dryness *in vacuo* giving a dark orange oil which was dried under high vacuum prior to purification by flash column chromatography using ethyl acetate–triethylamine (90%:10%) as the eluent. Yield = 63%. Found (required for C₈H₁₃NO): C, 68.59 (69.03); H, 9.34 (9.41); N, 10.34 (10.06)%. ¹H NMR (250 MHz, CDCl₃): δ 10.30 (1 H, s, CHO), 8.40 (1 H, broad s, phenolic proton), 7.40 (1 H, s, aryl CH), 7.00 (1 H, s, aryl CH), 3.55 (2 H, s, CH₂C₆H₂), 2.60 (2 H, t, MeNCH₂CH₂NEt₂), 2.55 (2 H, t, MeNCH₂CH₂NEt₂), 2.55 (4 H, q, NCH₂CH₃), 2.50 (4 H, q, NCH₂CH₃), 2.20 (3 H, s, NMe), 2.15 (3 H, s, CH₃C₆H₂) and 0.90 (6 H, t, NCH₂CH₃). ¹³C NMR (250 MHz, CDCl₃): δ 191.8 (CO), 159.6 (aryl), 136.6, 127.9, 127.8, 124.6, 122.7, 58.4, 54.3, 50.0, 46.7, 42.1 (NEt₂), 20.2 (NMe) and 11.0 (C₆H₂Me). IR (NaCl plates): 3480 (ν_{OH}), 2968, 2804 (ν_{C-H, aliphatic}) and 1679 cm⁻¹ (ν_{C=O}). MS (FAB⁺): *m/z* 278 (100%, [C₁₆H₂₆N₂O₂]⁺).

Unsymmetrical Schiff base proligand HL². The proligand **HL^B** (0.20 g, 0.746 mmol) was gently refluxed in ethanol (25 cm³) for approximately 10 min and *N,N*-dimethylethane-1,2-diamine (0.08 cm³, 0.746 mmol) added dropwise to the boiling solution *via* a microsyringe. The resulting solution was stirred for 10 minutes; the bright yellow solution was then cooled in ice before removal of the solvent *in vacuo* to give a bright yellow oil which was dried under a vacuum. Yield = 83%. Found (required for C₂₀H₃₆N₄O): C, 68.28 (68.92); H, 10.47 (10.47); N, 16.21 (16.07)%. ¹H NMR (250 MHz, CDCl₃): δ 8.35 (1 H, s, CHN),

Table 1 Crystal data, structure solution and refinement

	[Cu ₂ L ¹ Br ₃] 2	[Cu ₂ L ² (OH)][ClO ₄] ₂ 3	[NiL ^A (OH ₂) ₂][ClO ₄] ₂ ·4H ₂ O 4	[NiL ^C (OH ₂) ₂][ClO ₄] ₂ ·3CH ₃ OH 5
Chemical formula	C ₁₉ H ₃₃ Br ₃ Cu ₂ N ₄ O	C ₂₀ H ₃₆ Cl ₂ Cu ₂ N ₄ O ₁₀	C ₃₀ H ₅₈ Cl ₂ N ₄ Ni ₂ O ₁₈	C ₃₁ H ₅₈ Cl ₂ N ₄ Ni ₂ O ₁₇
Formula weight	700.30	690.51	951.12	947.13
<i>T</i> /K	150(2)	298(2)	150(2)	150(2) K
Crystal system, space group	Orthorhombic, <i>Pbca</i>	Monoclinic, <i>P2₁/c</i>	Monoclinic, <i>C2/c</i>	Triclinic, <i>P</i> $\bar{1}$
<i>a</i> /Å	15.282(3)	13.138(3)	22.938(6)	10.3948(15)
<i>b</i> /Å	11.3423(19)	12.800(4)	10.148(2)	10.6991(15)
<i>c</i> /Å	28.242(5)	18.132(5)	17.916(4)	10.8277(14)
<i>a</i> °				73.874
<i>β</i> °		107.870(10)	111.963(10)	85.768
<i>γ</i> °				62.618
<i>V</i> /Å ³	4895.4(14)	2902.1(14)	3867.8(16)	1025.2(2)
<i>Z</i>	8	4	4	1
<i>μ</i> /mm ^{−1}	6.653	1.705	1.193	1.124
Reflections collected	30453	6404	12499	4539
Independent reflections	5961 (<i>R</i> _{int} = 0.3510)	5118 (<i>R</i> _{int} = 0.0734)	4584 (<i>R</i> _{int} = 0.1299)	2938 (<i>R</i> _{int} = 0.0953)
Final <i>R</i> 1, <i>wR</i> 2 indices	0.0678, 0.1520	0.0688, 0.1724	0.1264, 0.3124	0.0892, 0.2436
[<i>I</i> > 2σ(<i>I</i>)] (all data)	0.1135, 0.1770	0.1055, 0.1988	0.2391, 0.3780	0.1126, 0.2946

7.15 (1 H, s, aryl CH), 6.95 (1 H, s, aryl CH), 3.65 (2 H, t, imineCH₂CH₂NMe₂), 3.55 (2 H, s, CH₂C₆H₂), 2.60 (2 H, t, imineCH₂CH₂NMe₂), 2.60 (2 H, t, MeNCH₂CH₂NET₂), 2.55 (2 H, t, MeNCH₂CH₂NET₂), 2.50 (4 H, q, NCH₂CH₃), 2.20 (6 H, s, NMe₂), 2.20 (3 H, s, NMe₂), 2.20 (3 H, s, CH₃C₆H₂), 0.90 (6 H, t, NCH₂CH₃). ¹³C NMR (250 MHz, CDCl₃): δ 165.1 (CN), 150.6 (aryl), 134.3, 130.2, 128.9, 123.2, 121.8, 59.9, 57.7, 55.8, 50.3, 45.8 (NMe₂), 42.8 (NET₂), 20.4 (NMe) and 11.2 (C₆H₂Me). IR (NaCl plates): 3405 (ν_{OH}), 2968, 2816 (ν_{C-H, aliphatic}) and 1635 cm^{−1} (ν_{C=N}). MS (FAB⁺): *m/z* 348 (30%, [C₂₀H₃₆N₄O]⁺).

Complexation reactions

Proligand HL¹ and CuBr₂. The proligand HL¹ (0.05 g, 0.15 mmol) was stirred at room temperature in methanol (20 cm³) with CuBr₂ (0.067 g, 0.3 mmol) for 1 hour. The dark green solution was hot filtered and the filtrate allowed slowly to evaporate at room temperature. A dark green crystalline solid was obtained, washed with light petroleum and left to dry in air at room temperature. Found for bulk sample (required for [C₁₉H₃₃Br₃Cu₂N₄O][CuBr₂]): C, 27.41 (27.05); H, 4.34 (4.94); N, 6.62 (6.64)%. IR (KBr disc): 1636 cm^{−1} (ν_{C=N}).

Proligand HL² and Cu(ClO₄)₂. The complex was prepared in a similar manner to that above using Cu(ClO₄)₂ (0.21 g, 0.575 mmol) and proligand HL² (0.10 g, 0.287 mmol). Found for bulk sample (required for [C₂₀H₃₇Cu₂N₄O₂][ClO₄]₂·3H₂O): C, 32.14 (32.26); H, 5.32 (5.56); N, 7.10 (7.52)%. IR (KBr disc): 3446 (ν_{O-H}), 1637 (ν_{C=N}), 1090, 625 cm^{−1} (ν_{ClO₄−}).

Proligand HL¹ and Ni(ClO₄)₂. Proligand HL¹ (0.05 g, 0.15 mmol) and nickel(II) perchlorate (0.110 g, 0.299 mmol) were stirred at room temperature in methanol (20 cm³) for 1 hour. The deep orange solution was hot filtered and the filtrate left slowly to evaporate at room temperature. A crystalline brown solid was obtained, washed with light petroleum (bp 60–80 °C) and dried in air. Recrystallisation from methanol gave green crystals suitable for structural analysis. Found (required for C₁₅H₂₉ClN₂NiO₉): C, 37.58 (37.89); H, 5.59 (6.15); N, 6.34 (5.89)%. IR (KBr disc): 3448 (ν_{OH}), 1628 (ν_{C=N}), 1083, 669 cm^{−1} (ν_{ClO₄−}).

Proligand HL² and Ni(ClO₄)₂. The complex was prepared in a similar manner to the above using Ni[ClO₄]₂·6H₂O (0.21 g, 0.575 mmol) and proligand HL² (0.10 g, 0.287 mmol). Found (required for C₃₁H₅₈Cl₂N₄Ni₂O₁₇): C, 38.61 (39.31); H, 5.67 (6.17); N, 5.28 (5.92)%. IR (KBr disc): 3446 (ν_{OH}), 1636 (ν_{C=N}), 1121, 624 cm^{−1} (ν_{ClO₄−}).

X-Ray crystallography

The details of the crystal data, and of the structure solution and refinement, are given in Table 1. Measurements were made on a Siemens SMART CCD area diffractometer for the copper complex **2** and the two nickel complexes **4** and **5**, and using a Siemens P4 four-circle diffractometer for **3**. The programs used were Siemens SMART and SAINT for control and integration software and SHELXTL as implemented on the Viglen Pentium computer; XSCANS was used for the P4.¹⁰

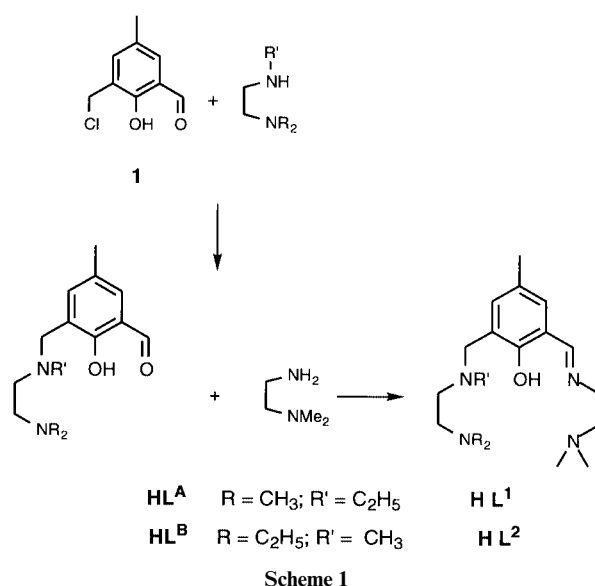
CCDC reference number 186/1945.

See <http://www.rsc.org/suppdata/doi/10.1039/B001395I> for crystallographic files in .cif format.

Results and discussion

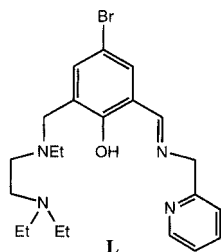
Synthesis and structural characterisation

The proligands (HL¹ and HL²) were synthesized from compound **1** by reaction with either *N*-ethyl-*N*',*N*'-dimethylethane-1,2-diamine or *N,N*-diethyl-*N*'-methylethane-1,2-diamine and *N,N*-dimethylethane-1,2-diamine according to Scheme 1 and

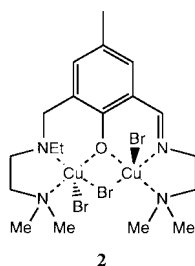


used to prepare homodinuclear copper(II) and nickel(II) complexes. Problems were encountered in obtaining reproducible pure bulk samples and so the complexes were recrystallised and the resulting products used in both structural and subsequent physico-chemical determinations.

The reaction of **HL**¹ with CuBr₂ in methanol gave a complex the bulk sample of which analysed as [Cu₃L¹Br₄]. This suggested that the product might contain the anion [CuBr₂]_n[−] to give either [Cu₃L¹Br₂][CuBr₂] or the dimer [Cu₂L¹Br₂]₂[Cu₂Br₄] by analogy with the crystallographically characterised product of the reaction of the unsymmetrical ligand **L** with CuBr₂ and



triethyl orthoformate in methanol, [CuLBr(HCO₂)]₂[Cu₂Br₄].⁵ In order to obtain this anion it was suggested that bromide ions present in solution reduce copper(II) to copper(I) and that the bromide ions are in turn oxidised to bromine. Copper(I) can then combine with bromide to give a linear anion, [CuBr₂][−], which can reversibly dimerise to give [Cu₂Br₄]^{2−} i.e. 2Cu^{II} + 6Br[−] → 2[CuBr₂][−] + Br₂; 2[CuBr₂][−] ⇌ [Cu₂Br₄]^{2−}. Both anions can be isolated from the solutions of copper(I) bromide depending on the nature of the cation present.^{11,12} A further possibility was that the product should be formulated as Cu₂L¹Br₃·CuBr. In order to resolve the ambiguity the bulk sample was recrystallised from methanol and crystal structure determinations were carried out which showed that the recrystallised complex was [Cu₂L¹Br₃] **2**. This suggests that the



bulk sample was [Cu₂L¹Br₃]CuBr and that CuBr had been loosely associated in the original precipitation.

The crystal structure of complex **2** was solved both at room temperature and at 150 K using different crystals from the recrystallised sample. The gross molecular features are found to be the same at both temperatures whereas there is a difference in the space group (*P*2₁/*c* at 293 K † and *Pbca* at 150 K) suggesting that a phase transition has occurred and that **2** is capable of existing in at least two polymorphic forms. The higher temperature structure is less accurate and so only the details of the structure solved at 150 K are discussed further.

The structure, illustrated in Fig. 3, confirms that complex **2** has the molecular formulation Cu₂L¹Br₃. The Cu...Cu separation of 3.221 Å is slightly longer than found in the structure of a related symmetrical dinuclear complex, 3.151 Å.¹³ The co-ordination environment at each copper atom is a square pyramidal arrangement derived from donor atoms (N₂Br₂O) from the ligand and the bromides. At Cu(1) the base of the pyramid stems from the N₂O compartment derived from the aminic side-arm of the ligand and a counter anionic non-bridging bromide, Br(1), with the bridging bromide, Br(2), providing the apex. At Cu(2) the base is derived from the N₂O compartment provided by the iminic side-arm of the ligand, with the fourth corner of the base occupied by the bridging bromide, Br(2); the apical co-

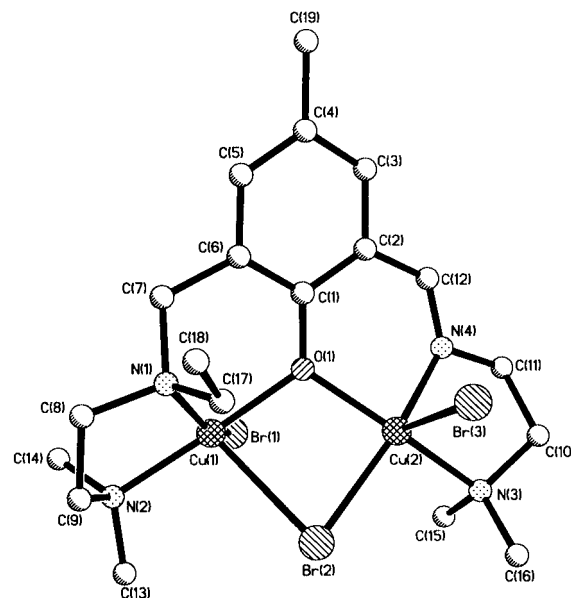


Fig. 3 The molecular structure of [Cu₂L¹Br₃] **2**. Selected bond lengths (Å) and angles (°) at the metal atoms: Cu(1)–O(1), 1.960(5); Cu(1)–N(2), 2.036(6); Cu(1)–N(1), 2.049(6); Cu(1)–Br(1), 2.4334(11); Cu(1)–Br(2), 2.6786(11); Cu(2)–O(1), 1.971(5); Cu(2)–N(4), 1.972(6); Cu(2)–N(3), 2.057(6); Cu(2)–Br(2), 2.4441(11); Cu(2)–Br(3), 2.6245(12); Cu(1)–Cu(2), 3.221; O(1)–Cu(2)–N(4), 88.4(2); O(1)–Cu(1)–N(2), 172.7(2); O(1)–Cu(2)–N(3), 159.4(2); O(1)–Cu(1)–N(1), 86.4(2); N(4)–Cu(2)–N(3), 83.3(2); N(2)–Cu(1)–N(1), 86.5(2); O(1)–Cu(2)–Br(2), 86.80(14); O(1)–Cu(1)–Br(1), 90.75(14); N(4)–Cu(2)–Br(2), 162.66(19); N(2)–Cu(1)–Br(1), 96.40(16); N(3)–Cu(2)–Br(2), 95.56(18); N(1)–Cu(1)–Br(1), 152.39(18); O(1)–Cu(2)–Br(3), 99.82(15); O(1)–Cu(1)–Br(2), 80.70(14); N(4)–Cu(2)–Br(3), 95.58(18); N(2)–Cu(1)–Br(2), 99.88(18); N(3)–Cu(2)–Br(3), 99.77(19); N(1)–Cu(1)–Br(2), 109.57(18); Br(2)–Cu(2)–Br(3), 101.65(4); Br(1)–Cu(1)–Br(2), 97.01(4); Cu(2)–Br(2)–Cu(1), 77.76(3); Cu(1)–O(1)–Cu(2), 110.1(2)°.

ordination site is supplied by a non-bridging bromide, Br(3). The two pyramids are not coplanar but are twisted at an angle of 90° to each other and the two non-bridging bromides Br(1) and Br(3) adopt a “*trans*” configuration with respect to each other.

Selected bond lengths and angles are shown in the caption to Fig. 3. Those associated with the ligand are normal, as has been found throughout the structural studies. The Cu(1)–O(1)–Cu(2) bridging angle is 110.1° for the endogenous bridge and there is a smaller angle of 77.8° for the Cu(1)–Br(2)–Cu(2) exogenous bridge. The Cu(1)–O(1) distance of 1.96 Å is slightly shorter than the Cu(2)–O(1) bond length of 1.97 Å. There is quite a marked difference between the two values of Cu–Br(2) for the two copper atoms; Cu(1)–Br(2) has a bond length of 2.68 Å compared to the Cu(2)–Br(2) bond length of 2.44 Å indicating an asymmetry found in the (μ-phenoxo)(μ-bromo) bridging unit. The two apical copper–bromide interactions are longer, Cu(1)–Br(2) 2.68 Å and Cu(2)–Br(3) 2.63 Å, than the equatorial copper–bromide distances, Cu(1)–Br(1) 2.43 Å and Cu(2)–Br(2) 2.44 Å. The Cu–N(iminic) bond length of 1.97 Å is 0.77 Å shorter than the Cu–N(aminic) bond and this closer approach may reflect a co-ordination preference that copper(II) may have for an unsaturated imine nitrogen compared to its saturated nitrogen counterpart. The index of the degree of trigonality (*τ*) within the structural continuum between square pyramidal, (*τ* = 0) and trigonal bipyramidal (*τ* = 1) geometries¹⁴ is 0.054 at Cu(2) and 0.34 at Cu(1) indicating that Cu(1) has a slightly more square pyramidal character than Cu(2).

Although crystals suitable for structural study were not recovered from the reaction of **HL**¹ with Cu[ClO₄]₂·6H₂O, crystals were obtained when the substitution pattern on the secondary amine was juxtaposed and *N,N*-diethyl-*N'*-methyl-ethane-1,2-diamine was used to produce **HL**². A structure was obtained and confirmed that the product of the complexation reaction was [Cu₂L²(OH)(ClO₄)]ClO₄ **3**. The crystal structure,

† *a* = 14.790(16), *b* = 15.400(13), *c* = 11.360(8) Å, β = 101.75(7)°, *V* = 2533(4) Å³.

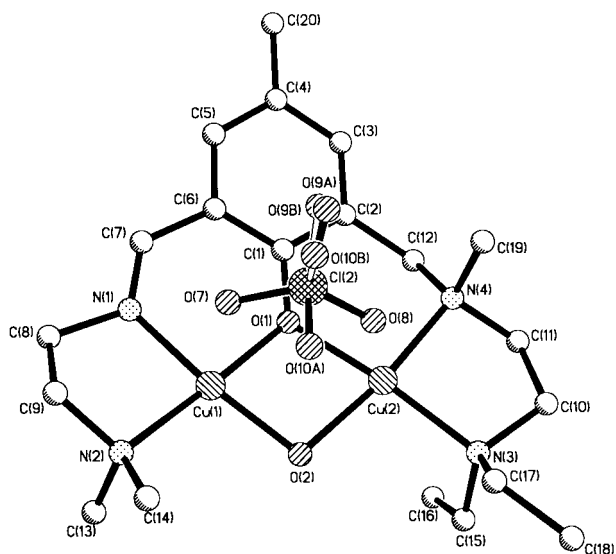
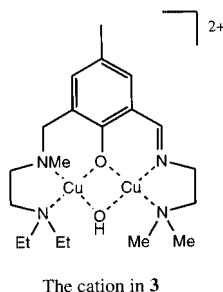


Fig. 4 The molecular structure of the cation in $[\text{Cu}_2\text{L}^2(\text{OH})(\text{ClO}_4)]\text{ClO}_4$ **3**. Selected bond lengths (Å) and angles (°) at the metal atoms: Cu(1)–O(2), 1.910(4); Cu(1)–N(2), 2.037(6); Cu(1)–O(1), 1.974(4); Cu(1)–N(1), 1.928(6); Cu(1)···Cu(2), 2.9596(13); Cu(2)–O(2), 1.940(4); Cu(2)–N(4), 2.005(5); Cu(2)–O(1), 1.979(4); and Cu(2)–N(3), 2.030(5); O(2)–Cu(1)–N(1), 169.5(2); O(2)–Cu(2)–O(1), 78.33(19); O(2)–Cu(1)–O(1), 79.16(19); O(2)–Cu(2)–N(4), 171.0(2); N(1)–Cu(1)–O(1), 91.7(2); O(1)–Cu(2)–N(4), 93.1(2); O(2)–Cu(1)–N(2), 103.1(2); O(2)–Cu(2)–N(3), 99.2(2); N(2)–Cu(1)–N(1), 86.0(2); O(1)–Cu(2)–N(3), 169.1(2); O(1)–Cu(1)–N(2), 177.6(2); N(4)–Cu(2)–N(3), 88.8(2); Cu(1)–O(1)–Cu(2), 96.96(19); and Cu(1)–O(2)–Cu(2), 100.5(2).



shown in Fig. 4 together with the numbering scheme, reveals the presence of a dinuclear core structure with a Cu···Cu internuclear separation of 2.96 Å. This is a closer internuclear approach than that found in the (μ-bromo) bridged complex **2** and reflects the smaller spatial requirements of the hydroxide anion relative to the bromide anion.

Selected bond lengths and angles are shown in the caption to Fig. 4. Those associated with the ligand are normal. Each copper atom has a square pyramidal arrangement of N_2O_3 donor atoms; the τ values are 0.13 for Cu(1) and 0.03 for Cu(2). The two nitrogens at Cu(1) are supplied by the iminic side-arm and at Cu(2) the two nitrogens are from the aminic pendant arm. The co-ordination environment at each metal is completed by the oxygen atoms from an endogenous μ-phenoxo bridge derived from the compartmental ligand itself, an exogenous μ-hydroxy bridge and an oxygen atom from a bridging bidentate perchlorate anion; Cu(1)–O(7) 2.53 and Cu(2)–O(8) 2.59 Å. Both of the perchlorate counter anions are somewhat disordered with a 47:53% occupancy at Cl(1) and a 46:54% occupancy at Cl(2). The double bridged (μ-phenoxo)(μ-hydroxy) unit was found to be slightly asymmetric with Cu(1)–O(1) 1.97, Cu(2)–O(1) 1.98, Cu(1)–O(2) 1.91 and Cu(2)–O(2) 1.94 Å. The close approach of the two metals gives rise to a small μ-phenoxo bridging angle of 97.0° and a hydroxy bridging angle of 100.5°.

In contrast to the reactions with Cu^{II} the reaction of **HL**¹ and **HL**² with $\text{Ni}(\text{ClO}_4)_2 \cdot 6\text{H}_2\text{O}$ in methanol followed by recrystal-

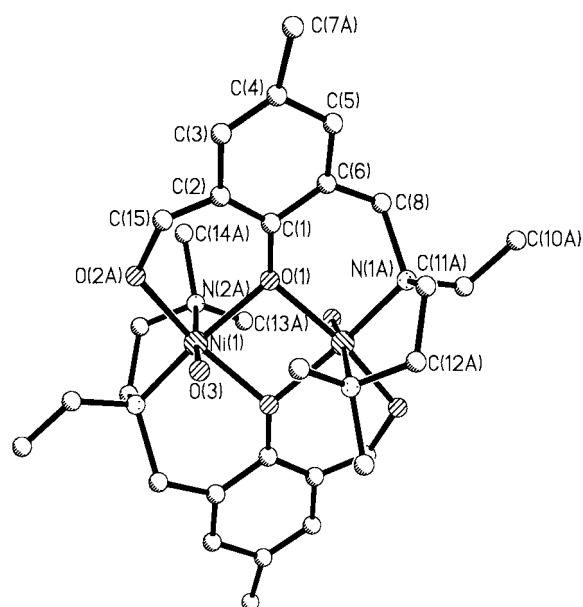
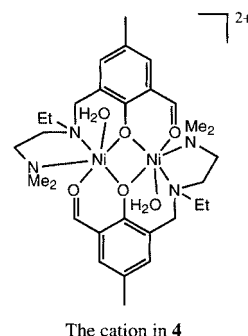


Fig. 5 The atom connectivity in the cation from $[\text{NiL}^{\text{A}}(\text{OH}_2)_2][\text{ClO}_4]_2 \cdot 4\text{H}_2\text{O}$ **4**.

lisation gave the complexes **4** and **5**. Instead of recovering μ-hydroxo-bridged dinuclear complexes, by analogy with the reaction of **HL**¹ and **HL**² with $\text{Cu}(\text{ClO}_4)_2 \cdot 6\text{H}_2\text{O}$, hydrolysis of the pendant Schiff base arm in the proligand has occurred. Recrystallisation of the complex from the reaction of **HL**¹ with $\text{Ni}(\text{ClO}_4)_2 \cdot 6\text{H}_2\text{O}$ gave a batch of green crystals.

The crystal structure showed that a dinuclear nickel(II) complex had been formed and that the imine bond of the unsymmetrical unsaturated proligand had undergone hydrolysis to give the corresponding aldehyde **HL**^A and that the complex was $[\text{NiL}^{\text{A}}(\text{OH}_2)_2][\text{ClO}_4]_2 \cdot 4\text{H}_2\text{O}$ **4**. The two molecules of the hydro-

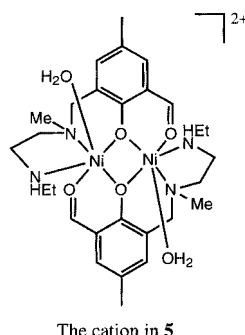


lysed ligand then assumed a typical octahedral arrangement around each nickel atom, resulting in a dimeric dinuclear nickel structure with a Ni···Ni distance of 3.088 Å. The molecular structure is shown in Fig. 5.

Each nickel atom is co-ordinated by the two nitrogen atoms from the saturated pendant arm moiety and the octahedral co-ordination at each metal is completed by interaction with the bridging phenolic oxygen atom, the carbonyl oxygen atom and an oxygen atom from a water molecule. The water molecules lie on either side of the ligand plane and so are “trans” to each other. The phenolic oxygen atoms serve as non-symmetric di(μ-phenoxo) bridges [Ni(1)–O(1)^{#1} 2.017(5), O(1)–Ni(1) 2.029(7) Å, Ni(1)^{#1}–O(1)–Ni(1) 99.5(3)°] between the two nickel atoms, and the perchlorate anions are not co-ordinated. There is considerable disorder in the cation and although this has caused difficulty with refinement of the bond lengths and angles to an acceptable level and has inhibited accurate determination of the molecular planes and dihedral angles pertinent to full interpretation of the magnetic data, the gross

stereochemical features of the complex are secure. The co-ordinating aminic arm, the methyl substituent on the phenyl ring and the keto-oxygen atom are disordered over two sites with a 56% occupancy of the major component; it is this major component that is depicted in Fig. 5. The perchlorate anion is disordered over two positions (52%:48%) and one water of solvation is also disordered.

The reason for the hydrolysis of the nickel complex on recrystallisation is not immediately apparent as the corresponding copper complexes recrystallise intact. It may be that the combination of a dinickel(II) metal centre, which could act as a focus for Lewis acid activity as in the proposed mechanism for the hydrolysis of urea by urease, and the use of a protic solvent like methanol encourages the hydrolysis. The acidity of the proton from any water molecule co-ordinated to the nickel would be enhanced so generating a nucleophile such as a hydroxide anion which could then attack the positive carbon of the imine bond and thus initiate a retro-Schiff base reaction. Furthermore the nickel(II) with its d^8 configuration strongly favours an octahedral environment and so in the presence of weakly co-ordinating perchlorate anions water can readily add to the empty axial sites provided by coplanar co-ordination by the ligand; this may then serve as a driving force for the hydrolysis. It is therefore possible that use of a polar aprotic solvent such as acetonitrile would discourage the hydrolysis reaction.



The reaction of **HL**² with $\text{Ni}[\text{ClO}_4]_2 \cdot 6\text{H}_2\text{O}$ in methanol followed by recrystallisation gave a further unexpected result. The preparation of the bulk sample followed that for the reaction of nickel with **HL**¹ with the IR spectrum of the product showing a peak at 1636 cm^{-1} , indicative of an imine bond. Recrystallisation of the bulk sample from methanol yielded crystals as green blocks suitable for X-ray diffraction studies. The crystal structure shown in Fig. 6 indicated that the sample has undergone hydrolysis giving a product **5** with a similar structure to that found for complex **4** but with the notable difference in that there is the loss of a C_2H_4 moiety from each of the terminal NEt_2 groups on the aminic pendant arm to give a secondary aminic HNEt functionality. The formulation of the complex is therefore $[\text{NiL}^{\text{C}}(\text{OH}_2)_2][\text{ClO}_4]_2 \cdot 3\text{CH}_3\text{OH}$. The reproducibility of the C_2H_4 loss is evidenced by the preparation and structural characterisation of an analogous complex, $[\text{NiL}^{\text{C}}(\text{NCCH}_3)_2][\text{BF}_4]_2 \cdot \text{CH}_3\text{CN}$, from the reaction of **HL**² with $\text{Ni}(\text{BF}_4)_2 \cdot n\text{H}_2\text{O}$ in methanol followed by recrystallisation from acetonitrile.¹⁵

Selected bond lengths and angles for the cation in complex **5** are given in the caption to Fig. 6. There is again an octahedral arrangement of N_2O_4 donors around each nickel atom supplied by two molecules of hydrolysed ligand and a water molecule. There are also three methanol molecules of solvation. The $\text{Ni} \cdots \text{Ni}$ internuclear distance is 3.107 \AA which compares favourably with 3.088 \AA for complex **4**. Each metal is doubly bridged by a non-symmetric di(μ -phenoxo) bridge from the hydrolysed ligand ($\text{Ni}-\text{O}$, $2.041(5)$ and $2.028(5)\text{ \AA}$). The co-ordination is completed by two sp^3 nitrogen donors from the aminic pendant arm ($\text{Ni}-\text{N}$, $2.090(6)$ and $2.100(6)\text{ \AA}$), an

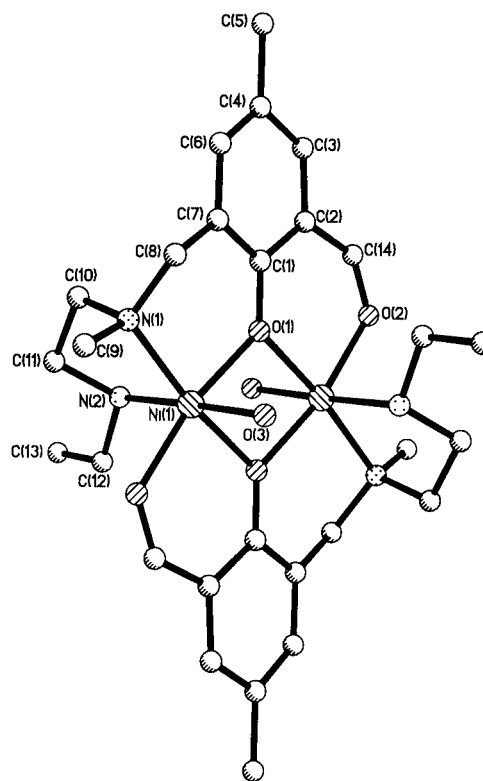


Fig. 6 The molecular structure of the cation in $[\text{NiL}^{\text{C}}(\text{OH}_2)_2][\text{ClO}_4]_2 \cdot 3\text{CH}_3\text{OH}$ **5**. Selected bond lengths (\AA) and angles ($^\circ$) at the metal atoms: $\text{Ni}(1)-\text{O}(1)$, $2.041(5)$; $\text{Ni}(1)-\text{O}(1)^{\#1}$, $2.028(5)$; $\text{Ni}(1)-\text{O}(2)^{\#1}$, $2.045(5)$; $\text{Ni}(1)-\text{N}(1)$, $2.090(6)$; $\text{Ni}(1)-\text{N}(2)$, $2.100(6)$; $\text{Ni}(1)-\text{O}(3)$, $2.143(5)$; and $\text{Ni}(1) \cdots \text{Ni}(1)^{\#1}$, 3.107 ; $\text{Ni}(1)^{\#1}-\text{O}(1)-\text{Ni}(1)$, $99.6(2)$; $\text{O}(1)^{\#1}-\text{Ni}(1)-\text{O}(1)$, $80.4(2)$; $\text{O}(1)^{\#1}-\text{Ni}(1)-\text{O}(2)^{\#1}$, $90.0(2)$; $\text{O}(1)-\text{Ni}(1)-\text{O}(2)^{\#1}$, $169.12(19)$; $\text{O}(1)^{\#1}-\text{Ni}(1)-\text{N}(1)$, $171.2(2)$; $\text{O}(1)-\text{Ni}(1)-\text{N}(1)$, $91.0(2)$; $\text{O}(2)^{\#1}-\text{Ni}(1)-\text{N}(1)$, $98.6(2)$; $\text{O}(1)^{\#1}-\text{Ni}(1)-\text{N}(2)$, $94.6(2)$; $\text{O}(1)-\text{Ni}(1)-\text{N}(2)$, $94.9(2)$; $\text{O}(2)^{\#1}-\text{Ni}(1)-\text{N}(2)$, $91.1(2)$; $\text{N}(1)-\text{Ni}(1)-\text{N}(2)$, $83.9(3)$; $\text{O}(1)^{\#1}-\text{Ni}(1)-\text{O}(3)$, $87.2(2)$; $\text{O}(1)-\text{Ni}(1)-\text{O}(3)$, $88.7(2)$; $\text{O}(2)^{\#1}-\text{Ni}(1)-\text{O}(3)$, $85.6(2)$; $\text{N}(1)-\text{Ni}(1)-\text{O}(3)$, $94.7(2)$; and $\text{N}(2)-\text{Ni}(1)-\text{O}(3)$, $176.2(2)$.

oxygen from the carbonyl group ($\text{Ni}-\text{O}$, $2.045(5)\text{ \AA}$) and an oxygen from a water molecule ($\text{Ni}-\text{O}$, $2.143(5)\text{ \AA}$).

Although the precise mechanism for this ligand degradation is not yet known it is possible to draw a parallel with observations made on the stability of the copper complexes of N,N,N',N' -tetraethylethane-1,2-diamine, $[\text{Cu}(\text{Et}_2\text{NCH}_2\text{CH}_2\text{NEt}_2)_2\text{Cl}_2]$ ¹⁶ and N,N,N',N' -tetrabenzylethane-1,2-diamine, $[\text{Cu}(\text{Bz}_2\text{NCH}_2\text{CH}_2\text{NBz}_2)_2\text{Cl}_2]$.¹⁷ These complexes have been found to undergo similar loss of a C_2H_4 moiety on recrystallisation to generate $[\text{Cu}(\text{Et}_2\text{NCH}_2\text{CH}_2\text{NHEt})\text{Cl}_2]$ and $[\text{Cu}(\text{Bz}_2\text{NCH}_2\text{CH}_2\text{NHBz})\text{Cl}_2]$. Acetaldehyde and benzaldehyde were detected as the respective accompanying products and a reduction-oxidation reaction proposed to occur. Interestingly this same reaction was not detected for N,N,N',N' -tetramethylethane-1,2-diamine $[\text{Cu}(\text{Me}_2\text{NCH}_2\text{CH}_2\text{NMe}_2)_2\text{Cl}_2]$ so paralleling the lack of activity at the NMe_2 pendant in complex **4**. It has also been suggested that the bulkier nature of the ethyl group relative to the methyl group can induce strain in the molecule and hence influence the reactivity. A further possibility is that either in the reaction carried out in methanol or during the process of slow crystallisation, with exposure to the atmosphere, the conditions have been set up for a Hofmann elimination reaction to occur. Protonation of the aminic arm, followed by nucleophilic attack by hydroxide anion, would then yield a secondary amine as observed (Scheme 2). The plausibility of the protonation step is illustrated by the ready protonation of the morpholino-arm in a mononuclear copper(II) complex of the unsymmetrical dinucleating ligand 4-bromo-2-(2-hydroxyethyliminomethyl)-6-(morpholin-4-yl-methyl)phenol (**HL**³).¹⁸

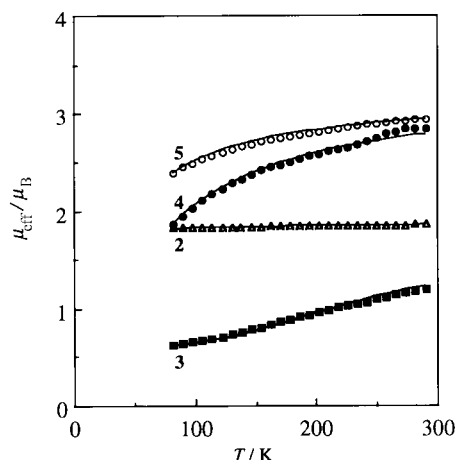
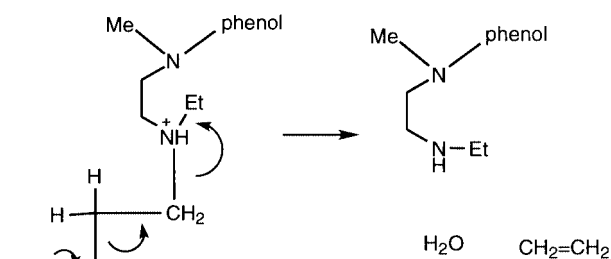
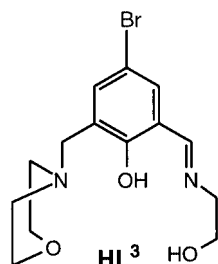


Fig. 7 μ_{eff} vs. T plots for compounds 2–5. Solid lines are drawn based on eqn. (1) for 2 and 3 and eqn. (2) for 4 and 5, using the magnetic parameters given in the text.



Scheme 2



The nature of the products confirmed by the structural studies draws attention to the instability of the nickel(II) complexes when left to stand in solution under ambient conditions or during redissolution for recrystallisation; in order to grow crystals of the complexes described herein it was necessary to leave the samples standing for many weeks. In the hydrolysis process the precursor aldehyde is regenerated and the nickel(II) complex of the precursor ligand is produced.

Properties

The physical measurements were carried out on recrystallised samples. The magnetic moment of complex 2 (per Cu atom) is $1.85 \mu_{\text{B}}$ at room temperature and the moment was practically independent of temperature down to liquid nitrogen temperature ($1.83 \mu_{\text{B}}$ at 82 K) (see Fig. 7). Evidently, no appreciable magnetic spin exchange operates between the pair of copper(II) ions in 2. On the other hand, the magnetic moment of 3 is subnormal at room temperature ($1.19 \mu_{\text{B}}$ per Cu) and decreases with decreasing temperature to $0.63 \mu_{\text{B}}$ at 82 K (Fig. 7). The result suggests the operation of an antiferromagnetic interaction between the copper(II) ions. Contamination with a significant amount of paramagnetic impurity is suggested from the χ_{A} vs. T curve showing a minimum around 120 K and an increasing tendency below this temperature. Magnetic analyses for 3 were therefore carried out using the modified Bleaney–

Bowers equation (1) where χ_{A} is the magnetic susceptibility per

$$\chi_{\text{A}} = \frac{N\beta^2 g^2}{kT} [3 + \exp(-2J/kT)]^{-1} (1 - \rho) + \rho \left(\frac{N\beta^2}{kT} \right) + N_{\text{a}} \quad (1)$$

Cu atom, N is Avogadro's number, β the Bohr magneton, k the Boltzmann constant, J the exchange integral, T the absolute temperature, N_{a} the temperature-independent paramagnetism and ρ the fraction of paramagnetic impurity. The paramagnetic impurity is presumed to be a monomeric copper(II) species. A tolerable magnetic fitting is obtained with this equation, using the magnetic parameters of $J = -215 \text{ cm}^{-1}$, $g = 2.10$, $N_{\text{a}} = 60 \times 10^{-6} \text{ cm}^3 \text{ mol}^{-1}$ and $\rho = 0.1$. The result clearly indicates a strong antiferromagnetic spin exchange in 3. The distinct magnetic properties of 2 and 3 can be explained by their different core structures. In the case of 2 both Cu(1) and Cu(2) have a square-pyramidal geometry sharing the phenolic oxygen O(1) and the bridging bromide ion Br(2). The basal plane for Cu(1) is formed by O(1), N(1), N(2) and Br(1), and Br(2) occupies the apical site but the basal plane for Cu(2) is formed by O(1), Br(2), N(3) and N(4) with terminal Br(3) occupying the apical site. The O(1) can contribute to an antiferromagnetic exchange but Br(1) contributes to a ferromagnetic exchange between the two copper ions. This is an example of counter-complementarity of the bridging groups in a doubly bridged dinuclear copper(II) complex, and the overall magnetic interaction of this complex is very weakly antiferromagnetic.

In the case of complex 3 the two bridging oxygens, O(1) and O(2), are shared at the equatorial positions of Cu(1) and Cu(2). This is an example of complementarity of bridging groups, and the two oxygens contribute to an antiferromagnetic spin exchange to produce a strong antiferromagnetic interaction ($J = -215 \text{ cm}^{-1}$). Both complexes showed only a broad EPR signal centered around $g = 2.0$ when measured as powdered samples; the broadening is assigned to a dipolar interaction in 2 and to spin exchange in 3.

Complexes 2 and 3 are also differentiated by our preliminary cyclic voltammetric studies (using a glassy carbon electrode in dmf and a Ag–AgCl reference electrode). Complex 2 shows a quasi-reversible couple at -0.03 V (vs. Ag–AgCl) [$E_{\text{pc}} = -0.10 \text{ V}$ and $E_{\text{pa}} = +0.04 \text{ V}$] and a reversible couple at -0.85 V [$E_{\text{pc}} = -0.90 \text{ V}$ and $E_{\text{pa}} = -0.80 \text{ V}$]. These can be attributed to stepwise reductions at the metal centre, $\text{Cu}^{\text{II}}\text{Cu}^{\text{II}} \rightarrow \text{Cu}^{\text{II}}\text{Cu}^{\text{I}}$ and $\text{Cu}^{\text{II}}\text{Cu}^{\text{I}} \rightarrow \text{Cu}^{\text{I}}\text{Cu}^{\text{I}}$, respectively. Complex 3 shows a weak couple at -0.30 V and an irreversible couple near -0.9 V . The former can be ascribed to the monomeric copper impurity. Owing to the irreversible nature of the wave near -0.9 V and the presence of the monomeric impurity, we could not determine the number of electrons transferred at -0.9 V . The facile reduction of 2 relative to 3 certainly relates to the square-pyramidal geometry about the Cu atoms in 2 and the involvement of the soft donor Br^- anion. The reduction of the Cu atoms of 3 is more difficult because the square-planar environment about the metals is an unfavourable geometric environment for Cu^{I} .

The room-temperature magnetic moments for complexes 4 and 5 (per Ni atom) are 2.85 and $2.94 \mu_{\text{B}}$, respectively, which are compared to the spin-only value for isolated nickel(II) atoms of $2.83 \mu_{\text{B}}$. The moments gradually decreased with decreasing temperature to 1.85 and $2.39 \mu_{\text{B}}$, respectively, at 82 K, suggesting an antiferromagnetic spin-exchange interaction within each molecule (Fig. 7). Magnetic analyses were carried out using the magnetic susceptibility expression (2) for an ($S_1 = 1$)–($S_2 = 1$)

$$\chi_{\text{A}} = \frac{(Ng^2\beta^2/3kT)[5 + \exp(-4J/kT)]}{[5 + 3\exp(-4J/kT) + \exp(-6J/kT)]} + N_{\text{a}} \quad (2)$$

system based on the Heisenberg model. Fairly good magnetic

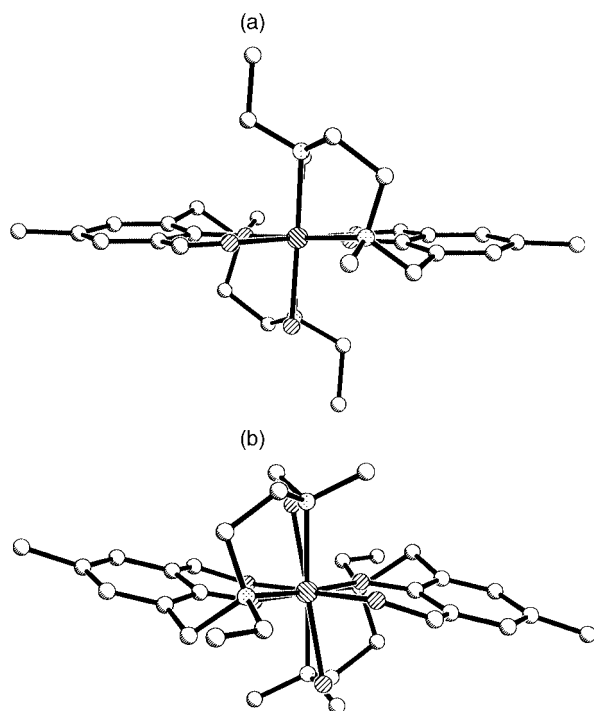
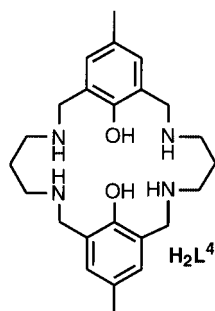


Fig. 8 The dinickel complexes viewed along the Ni...Ni vector: (a) **5** and (b) the major component of **4**.

simulations are obtained with this equation, as seen in Fig. 7, using magnetic parameters of $J = -31 \text{ cm}^{-1}$, $g = 2.15$, $N_a = 200 \times 10^{-6} \text{ cm}^3 \text{ mol}^{-1}$ for **4** and $J = -17 \text{ cm}^{-1}$, $g = 2.15$, $N_a = 200 \times 10^{-6} \text{ cm}^3 \text{ mol}^{-1}$ for **5**.

Thompson and co-workers have studied the magnetostructural correlation for di(μ -phenoxo)dinickel(II) complexes derived from the macrocyclic ligand H_2L^4 and reported a linear



relationship between the Ni–O–Ni bridging angle and the exchange integral ($-J$); the larger the Ni–O–Ni angle the stronger is the antiferromagnetic interaction.¹⁹ The complexes **4** and **5** significantly differ in exchange integral (-31 and -17 cm^{-1} respectively) (in spite of their similar Ni–O–Ni angles (99.5 and 99.6° respectively)). The equatorial ligating atoms and nickel atoms in **5** are essentially coplanar (Fig. 8a) and the exchange integral can be incorporated into the above linear relationship. However for **4** it is possible that there are other factors influencing the deviation from the relationship. The disordered nature of the structure precludes an accurate determination of the dihedral angles and planarities at the dinuclear centre but there is a distinct “stepping” of the conformation of **4** which leads to distortion of the equatorial environments at the nickel atoms (Fig. 8b).

Conclusion

The reaction of copper(II) with the unsymmetric Schiff bases HL^1 and HL^2 gave homodinuclear complexes. The structure of $[\text{Cu}_2\text{L}^1\text{Br}]$ **2** revealed that the asymmetry in the molecule was not restricted to that implicit to the ligand (donor asymmetry) but that the two square-pyramidal arrangements at the copper atoms were subtly different with the bridging Br(2) atom serving as the apex for the geometrical arrangement at Cu(1) and a corner of the pyramidal base at Cu(2) leading to a non-coplanarity of the two square pyramids. This distortion was reflected in the magnetic properties of **2**, no antiferromagnetic coupling being detected between the two Cu atoms. A strong antiferromagnetic coupling ($J = -215 \text{ cm}^{-1}$) was observed in complex $[\text{Cu}_2\text{L}^2(\text{OH})(\text{ClO}_4)]\text{ClO}_4$ **3**, where the presence of the hydroxy bridge, complementary to the phenoxy bridge, aids coupling. The reactions of HL^1 and HL^2 with nickel(II) led to hydrolysis reactions in which the pendant Schiff base was cleaved; with HL^1 the homodinuclear complex $[\text{NiL}^A(\text{OH}_2)]_2 \cdot [\text{ClO}_4]_2 \cdot 4\text{H}_2\text{O}$ was formed and with HL^2 hydrolysis was followed by elimination of an C_2H_4 moiety from one C_2H_5 of the terminal NET_2 group of the iminic side arm to leave a NHet group and the dinuclear complex $[\text{NiL}^C(\text{OH}_2)]_2[\text{ClO}_4]_2 \cdot 3\text{CH}_3\text{OH}$.

Acknowledgements

We thank the EPSRC for a studentship (to S. R. H.) and for funds towards the purchase of the diffractometer; we also thank the British Council and the Daiwa Anglo-Japanese Foundation for their support and the Japanese Ministry of Education for the award of a Monbusho Research Experience Fellowship for Young Foreign Researchers (to S. R. H.).

References

- 1 D. E. Fenton and H. Okawa, *Chem. Ber./Recueil*, 1997, **130**, 433 and references therein.
- 2 T. N. Sorrell, *Tetrahedron*, 1989, **45**, 3.
- 3 J. H. Satcher, Jr., M. W. Droegge, T. J. R. Weakley and R. T. Taylor, *Inorg. Chem.*, 1995, **34**, 3317.
- 4 D. E. Fenton, *Adv. Inorg. Bioinorg. Mech.*, 1983, **2**, 187.
- 5 J. D. Crane, D. E. Fenton, J. M. Latour and A. J. Smith, *J. Chem. Soc., Dalton Trans.*, 1991, 2979.
- 6 M. Lubben, R. Hage, A. Meetsma, K. Byma and B. L. Feringa, *Inorg. Chem.*, 1995, **34**, 2217.
- 7 J. Reim and B. Krebs, *J. Chem. Soc., Dalton Trans.*, 1997, 3793.
- 8 E. Lambert, B. Chabut, S. Chardon-Noblat, A. Deronzier, G. Chottard, A. Bousseksou, J.-P. Tuchagues, J. Laugier, M. Dardet and J.-M. Latour, *J. Am. Chem. Soc.*, 1997, **119**, 9424.
- 9 S. Uozumi, M. Ohba, H. Okawa and D. E. Fenton, *Chem. Lett.*, 1997, 673.
- 10 SHELXTL, An integrated system for solving and refining crystal structures from diffraction data (Revision 5.1), Bruker AXS LTD, Madison, WI, USA, 1997.
- 11 M. Asplund and S. Jagner, *Acta Chem. Scand., Ser. A*, 1984, **38**, 135.
- 12 M. Asplund, S. Jagner and N. Nilsson, *Acta Chem. Scand., Ser. A*, 1983, **37**, 57.
- 13 C. J. O'Connor, D. Firmin, A. K. Pant, B. R. Babu and E. D. Stevens, *Inorg. Chem.*, 1986, **25**, 3000.
- 14 A. W. Addison, T. N. Rao, J. Reedijk, J. van Rijn and G. C. Verschoor, *J. Chem. Soc., Dalton Trans.*, 1984, 1349.
- 15 S. Clunas and D. E. Fenton, unpublished work.
- 16 R. C. E. Belford, D. E. Fenton and M. R. Truter, *J. Chem. Soc., Dalton Trans.*, 1972, 2345.
- 17 K. C. Patel, S. R. Shirali and D. E. Goldberg, *J. Inorg. Nucl. Chem.*, 1975, **37**, 1659.
- 18 H. Adams, N. A. Bailey, D. E. Fenton and G. Papageorgiou, *J. Chem. Soc., Dalton Trans.*, 1995, 1883.
- 19 K. K. Nanda, L. K. Thompson, J. N. Bridson and K. Nag, *J. Chem. Soc., Chem. Commun.*, 1994, 1337.